Electronic Appendix

Table S1

Major oxides and Th and U concentrations in host rocks of the Agua Blanca Fault.

	UTM Coordinates Zone 11 north		Rock		SiO_2	Na_2O	K_2O	Th	U
Sample	East (m)	North (m)	Classification	Texture	wt. %	wt. %	wt. %	µg g^{-1}	µg g^{-1}
1	552875	3500105	Granodiorite	Subhedral	67.12	3.85	1.60	3.57	1.12
2	551083	3493207	Tonalite	Granophyric	74.15	4.62	2.95	5.01	1.66
3	565473	3481183	Tonalite	Anhedral	72.00	5.23	0.39	6.64	1.78
4	582128	3474492	Granodiorite	Anhedral	68.27	4.16	0.86	2.10	1.06
5	582128	3474492	Diorite	Anhedral	51.97	2.67	0.46	0.39	0.25
6	615226	3472029	Tonalite	Anhedral	73.02	3.25	3.35	10.79	1.12
7	610414	3469310	Tonalite	Anhedral	70.85	3.99	1.24	7.42	0.93
8	618055	3474837	Granodiorite	Anhedral	64.47	3.16	1.97	9.60	1.45
9	589920	3494031	Diorite	Anhedral	52.09	2.53	0.53	0.86	0.32
10	590288	3495267	Tonalite	Porphyritic	71.98	3.31	2.45	7.58	2.10
11	529140	3508979	Dacite	Porphyritic	66.21	5.18	1.49	2.72	1.02
12	526947	3508973	Dacite	Porphyritic	67.15	4.95	1.50	3.02	1.09
13	529136	3510321	Rhyolite	Porphyritic	71.83	5.29	2.09	4.44	1.66
							Mean	4.93	1.20

Table S2

UTM zone 11 north coordinates of the thermal water samples. Delta values of $\delta^{18}O_c$ and δ^2H_c of thermal waters corrected by the seawater fraction (F_{SW}). Silica concentration (SiO_{2c}, mg L^{-1}) and theoretical discharge temperature ($T_{unmixed}$) of the coastal–submarine waters corrected by the admixture of seawater. We assume an average seawater fraction of 0.4 for the LJB site to estimate their unmixed maximum temperature.

Sample	East (m)	North (m)	Cl/Br	F_{SW}	$\delta^{18}O_c$	δ^2H_c	SiO_{2c}	$T_{discharge}$ (°C)	$T_{unmixed}$ (°C)
VT	615837	3473247							
SV	582088	3474309							
ST	575557	3492303							
UR	553554	3499807	333						
AJ	553158	3494074	338						
W368	531918	3508928	313	0.26	-7.2	-50.0	63.7	50	61
W369	532196	3508954	273	0.25	-6.9	-46.9	90.8	73	91
W363	531822	3509108		0.26	-7.6	-50.0	99.8	30	34
W2014	531788	3508969		0.26	-7.6	-51.5	84.1	29	33
W367	531834	3508987		0.26	-7.7	-50.2	100.9	38	45
WAGC	532105	3509279		0.29	-7.2	-47.9	119.4	45	56
LJB-a	532015	3509371	327	0.41	-6.9	-51.5	138.3	50	72
LJB-b	532030	3509375	340	0.39	-6.3	-47.3	141.6	55	78
LJB-c	532007	3509373	294	0.33	-7.5	-49.3	129.2	60	80
LJB-d	531964	3509358	273	0.48	-7.7	-53.1	100.1	46	71
LJB				0.40				94	144
SMF	526231	3509665		0.57	-7.2	-55.0	359.2	102	212

Table S3

Classical geothermometric temperatures are reported. Temperatures estimated with T_{quartz} and $T_{chalcedony}$ geothermometers use the SiO_2 concentration corrected for mixing with seawater. Values of variables (T_{Geot} and $\Delta T/\Delta z$) used in Eq. (14) to estimate the minimum depth of equilibration ($z_{eq,min}$) along the Agua Blanca Fault. For the estimation of $z_{eq,min}$ in the La Jolla beach area we used the maximum geothermometric temperature of LJB-b.

Sample	$T_{Na/K}$ (°C)	T_{quartz} (°C)	$T_{chalcedony}$ (°C)	T_{Geot} (°C)	BDTZ[a] (km)	$\Delta T/\Delta z$ (°C/km)	$z_{eq,min}$ (km)
VT	105	105	75	105	16	17.3	5.1
SV	103	98	68	103	15	18.7	4.6
ST	108	94	63	108	15	18.7	4.9
UR	112	105	75	112	15	18.7	5.1
AJ	121	96	65	121	15	18.7	5.6
W368	168	113	84				
W369	181	132	104				
W363	168	137	110				
W2014	162	128	99				
W367	172	138	110				
WAGC	170	147	121				
LJB-a	163	156	131				
LJB-b	165	158	133	158	12	24.0	5.9
LJB-c	169	152	126				
LJB-d	163	137	110				
SMF	214	228	209	228	12	24.0	8.8

[a] Brittle–ductile transition

Table S4

Elevation difference (Δh) and distance (Δl) between meteoric water recharge and discharge as hot springs, resulting in a hydraulic head gradient.

Sample	Discharge (m a.s.l)	Recharge (m a.s.l)	Recharge horizontal distance (m; Δl)	Hydraulic head difference (m; Δh)	Hydraulic head gradient ($\Delta h/\Delta l$)
VT	734	1300	18000	566	0.031
SV	215	930	30000	715	0.024
ST	498	1220	11000	722	0.066
UR	203	870	20000	667	0.033
AJ	130	780	11000	650	0.059
LJB-b	0	770	8300	770	0.093
SMF	-30	760	12500	790	0.063

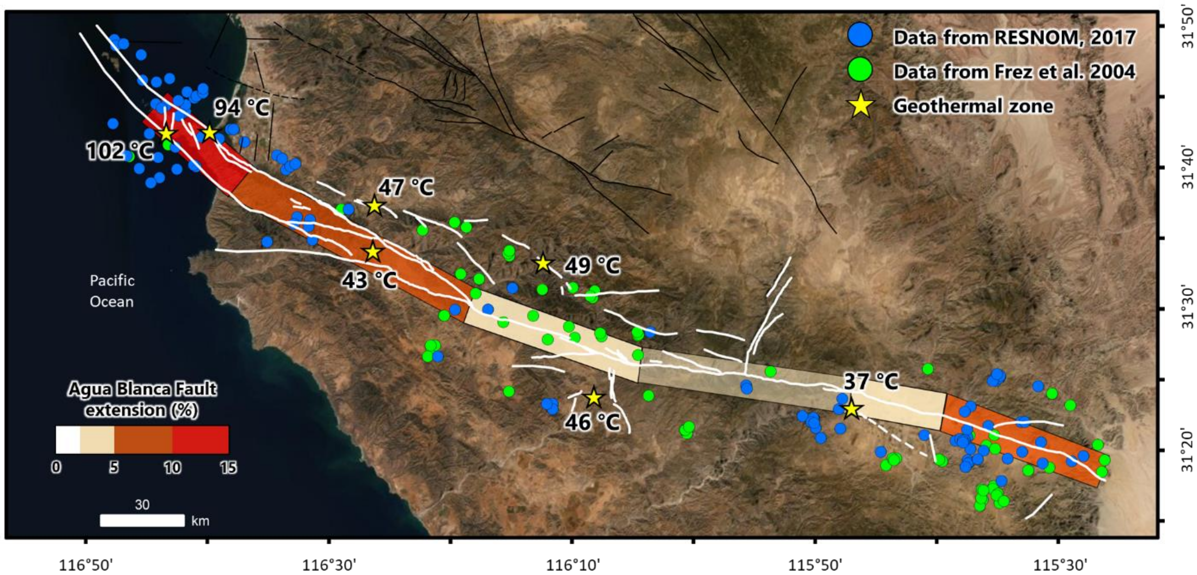

Figure S1. Seismic epicenters occurred along the Agua Blanca Fault, Baja California, Mexico (Frez et al., 2004; RESNOM, 2017). Colored bands along the Agua Blanca Fault show the extension as a fraction of total displacement (%) along five geographic segments of the fault (Wetmore et al., 2019).

References

Frez, J., Acosta, J., Nava, A., Suarez, F., Gonzalez, J., Arellano, G., et al. (2004). Microseismicity Studies in Northern Baja California, Mexico: the Agua Blanca Fault. AGU. Retrieved from https://ui.adsabs.harvard.edu/abs/2004AGUFM.S51A0129F/abstract

RESNOM. (2017). Red Sísmica del Noroeste de México. https://doi.org/10.7914/SN/BC

Wetmore, P. H., Malservisi, R., Fletcher, J. M., Alsleben, H., Wilson, J., Callihan, S., et al. (2019). Slip history and the role of the Agua Blanca fault in the tectonics of the North American-Pacific plate boundary of southern California, USA and Baja California, Mexico. *Geosphere*, *15*(1), 119–145. https://doi.org/10.1130/GES01670.1